SIAM J. APPL. MATH.
Vol. 50, No. 4, pp. 943-955, June 1990

A PERIOD-ADDING PHENOMENON*

MARK LEVI†

Abstract. A simple geometrical explanation is given for the "period-adding" phenomenon observed in the 1927 experiment of van der Pol and van der Mark and refined recently by Chua and Kennedy. The problem is reduced to a simple circle map. In the second part of the paper some previous results are outlined to show how the same phenomenon arises in a class of van der Pol-type systems with periodic forcing, and in conclusion some recent topological results are applied to such systems.

Key words. circle maps, period adding

AMS(MOS) subject classifications. 34C, 58F, 94C

1. Introduction. In this paper we use a geometrical approach to explain the period-adding on two examples, one a neon tube circuit studied experimentally in 1927 by van der Pol and van der Mark and very recently by Kennedy and Chua [18], and the other a class of van der Pol-type equations. Period-adding phenomena manifest themselves in the additive rather than multiplicative changes of periods of periodic solutions. Perhaps the earliest observation of this phenomenon (described in detail in the next section), due to van der Pol and van der Mark [29], dates back to 1927, as was pointed out by Chua.

In recent years, period-adding has been observed in some real-life systems, in particular, in the Belousov–Zhabotinsky reaction-diffusion equation [27], [28], and in various electronic oscillators other than van der Pol's [6]. Pikovsky [26] has given a simple one-dimensional mapping that models the behavior of the Belousov–Zhabotinsky system and where the period-adding effect is geometrically transparent. Kaneko [16] has studied the standard circle map and observed some period-adding behavior. It should be pointed out that the standard van der Pol equation in the relaxation case and with periodic forcing exhibits period-adding as well, as described below. This was well known in the early 1940s from the work of Cartwright and Littlewood [20].

Despite the considerable interest in the subject, there seems to have been no rigorous geometrical study of period-adding in a *differential equation.* In this paper we give a simple geometrical (and rigorous) explanation of the phenomenon first discovered in the 1927 experiment of van der Pol and van der Mark [29], repeated with greater precision by Kennedy and Chua [18], by deriving dynamical equations and analyzing them geometrically. We also point out how some results of Cartwright and Littlewood can be interpreted in terms of period adding and restate some topological explanations of the behavior in the van der Pol-type systems.

Our analysis illustrates the fact that period-adding is due to a certain hidden but simple *near periodic dependence of a certain return map on the parameter.* As it turns out, a circle map associated with the Poincaré map has the property that its image rotates with the change of parameter. We give a geometrical explanation of this rotational property in two types of differential equations. This phenomenon was explained before for one of these two types.

* Received by the editors December 2, 1988; accepted for publication June 20, 1989.

† Mathematics Department, Stanford University, Stanford, California 94305. This research was supported in part by the Air Force Office of Scientific Research and by the Defense Advanced Research Projects Agency.

Period-adding occurs on a larger scale both in parameter and in phase space than the period-doubling, as will be shown below. Actually, period-doubling sequence (together with many other bifurcations) is embedded in the gaps between the period-adding plateaus in the first of our two examples. In that sense it is a macroscopic, or global phenomenon.

Many details of experimental observations will be explained by a simple circle map using geometro-analytical arguments, answering, among others, the following questions:

- Why do periods change additively, i.e., increase by a fixed multiple of the forcing period T—in the two examples below, by $2T$ and T, respectively—when a parameter crosses certain nearly equally spaced short bifurcation intervals?
- Why is noise observed in these short intervals?
- Why do stable periodic solutions have odd periods?
- What is the geometrical reason for the existence of the "Angel's staircase"?
- What causes the gaps between the steps for one parameter range and the overlaps for another (Fig. 1(c))?

2. Background, results, and open problems. The first published account of the effect appeared in 1927 and is due to van der Pol and van der Mark [29], who considered a periodically forced relaxation oscillator depicted in Fig. 1(a). The neon tube's I-V characteristic is a nonsingle-valued function depicted in Fig. 1(b). Resistance R was chosen large, and parameters C, R were adjusted in such a way that the frequency of unforced oscillations coincided with the forcing frequency (50Hz). In the absence of periodic forcing, the current seeps through the very large resistor slowly charging the capacitor (the relaxation stage). Once the voltage on the capacitor exceeds the threshold, the neon tube's resistance drops and the capacitor quickly discharges causing a flash of light, whereas the cycle begins anew.

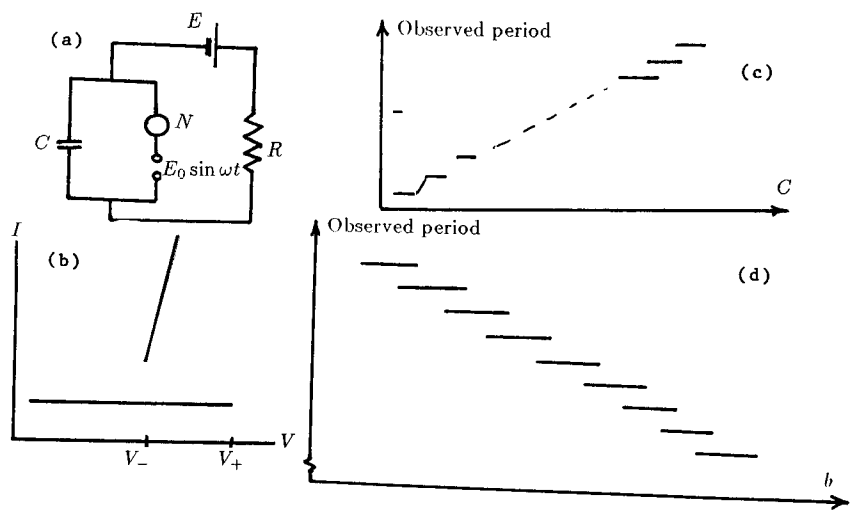

FIG. 1. (a) *The relaxation oscillator of van der Pol and ver der Mark.* (b). *The neon tube's I-V characteristic.* (c) *Observed periods dependence on the capacitance in the neon tube oscillator.* (d) *Observed period's dependence on the forcing amplitude b in equation* (1).

While increasing C from its initial value, van der Pol and van der Mark observed a "period-adding staircase" sketched in Fig. 1(c), where the periods increase by the

same amount at each jump, rather than double. The staircase contained approximately 40 steps, and unlike the period-doubling sequence, its plateaus did not follow the Feigenbaum ratio and were of roughly comparable lengths. For that reason we could call this an "Angel's staircase." Another feature of the Angel's staircase in Fig. 1(c) is the existence of gaps for low values of C, narrowing for larger values and giving way to the overlapping of plateaus, resulting in hysteresis. In § 3 we will explain these phenomena after deriving equations for the circuit. It is an interesting problem as to the specifics, perhaps computer-assisted, of a similar explanation for the recent new examples of [6] and [25]. It should be pointed out that there has been no explanation for some more complex patterns, such as the appearance of Farey trees in the oscillation patterns [21].

A very similar behavior is observed in another relaxation oscillator (triode coupled to an RLC circuit with positive feedback) with periodic forcing, now carrying the name of van der Pol:

$$\varepsilon\ddot{x}+(x^2-1)\dot{x}+\varepsilon x = b\sin t. \tag{1}$$

Here ε is small but fixed and b is the forcing amplitude, which will be the variable parameter of interest. Electronic experiments on this system showed that as the forcing amplitude b was increased through the interval $(0, \frac{2}{3})$, the following behavior occurred (Fig. 1).

First, a periodic solution was observed whose period $(2n+1)2\pi$, $n>0$ an integer, was an odd multiple of the period 2π of the forcing term.

This odd period persists as b increases through the interval A_1, (Fig. 1) until the periodic solution disappears and is replaced by noise in the short "chaotic" gap C_1. In the next interval B_1 the noise is replaced by another periodic motion of odd period $(2n-1)2\pi$ two forcing periods shorter than the previous period. This pattern $(\cdots A, C, B, C, A, \cdots)$ continues until b comes close to $\frac{2}{3}$. For $b>\frac{2}{3}$ we observe the 1:1 lock-in, i.e., the (globally attracting) periodic solution of the same period as the driving term. If b is decreased back through the intervals B, C, A, we observe a hysteresis phenomenon: on the way down in each B-gap we see a $(2n-1)T$-periodic solution whose odd period is $2T$ shorter than on the way up (Fig. 1).

In §§ 4 and 5 we will give a short exposition of the earlier explanation [19] of this phenomenon for the class of systems

$$\varepsilon\ddot{x}+\phi(x)\dot{x}+\varepsilon x = bp(t) \tag{2}$$

similar to van der Pol's equation (1) but with the damping and forcing terms modified to preserve the qualitative behavior while at the same time allowing for a rigorous analysis. It seems rather clear from numerical evidence and from heuristic arguments that the modified equations (2) have the same qualitative behavior as the classical van der Pol equation (1). Our modification consists of the requirement that both ϕ and p be greater than a certain constant (say, 1) outside sufficiently small neighborhoods of their zeros. We will further insist that the symmetry properties of $\phi(x)$ and $p(t)$ be the same as in the original van der Pol equation (1): $\phi(x)$ is even, $p(t)$ is T-periodic, odd, and satisfying $p(t+T/2)=-p(t)$ (odd with respect to $t=T/2$), $p(t)>0$ for $0<t<T/2$ and $\phi(x)<(>)0$ for $|x|<(>)1$.

All the proofs for the statements in §§ 4 and 5 can be found in [19] together with various other aspects of the problem, such as the description of chaotic behavior via symbolic dynamics, bifurcations, structural stability, etc.

It is a difficult and important problem to do the same analysis for (1). There is the famous work of Cartwright and Littlewood [20], and some very interesting

asymptotic results of Grasman and others [9], but no rigorous proofs for the full picture are available. There are finer features in the period-adding sequence that were observed in electronic, numerical, and chemical experiments [6], [18], [21], [28]. These questions will be addressed elsewhere.

3. Period-adding in the neon tube relaxation circuit.

3.1. Derivation of the equations. With the notation of Fig. 1(a), we obtain, using Kirchhoff's laws:

$$-E+(i_1+i_2)R+V=0 \tag{3}$$

$$V=i_2R_N+E_\omega, \tag{4}$$

where $V=C^{-1}q_1$ is the voltage on the capacitor, q_1 = the charge, $\dot{q}_1=i_1$, $E_\omega=E_\omega(t)=E_\omega(t+T)$ is the externally imposed periodically changing voltage, and R_N = resistance of the neon tube, which is the function of the voltage applied to the tube as shown in Fig. 1. Since that voltage is $W\equiv V-E_\omega$, we have $R_N=R_N(W)$.

Substitution of (4) into (3) gives

$$-E+\left[i_1+\frac{V-E_\omega}{R_N}\right]R+V=0.$$

Using $i_1=\dot{q}_1=C\dot{V}$, we obtain the desired equation

$$C\dot{V}+\left(\frac{1}{R}+\frac{1}{R_N}\right)V=\frac{E}{R}+\frac{E_\omega(t)}{R_N}, \tag{5}$$

where $R_N=R_N(W)=R_N(V-E_\omega)$ is the nonlinearity.

3.2. Geometric discussion of the dynamics. To analyze (5) it suffices to understand the form of the Poincaré map $P: V_{t=0}\mapsto V_{t=T}$ ($T=2\pi/\omega$ being the period of $E_\omega(t)$), and its dependence on C. The finer details of the shape of P will be studied elsewhere.[1] Nevertheless, the mechanism of period-adding can be explained with only partial information on P. The associated circle map turns out to have a near-periodic dependence on C, with periodic change resulting in an increase of the period by one.

To make this more explicit, we begin with *the autonomous case.* Our first important observation is that the phase space of (5) is not a line, but a "Riemann line," consisting of two rays $\{V: -\infty<V\leqq V_+\}$ and $\{V: V_-<V<\infty\}$, (Fig. 2). This is due to the nonsingle-valued character of R_N: for $V_-\leqq V\leqq V_+$ the neon tube may be either *on* or *off*, i.e., we may have $R_N(V)=\infty$ (tube is *off*) or $R_N=R_c<\infty$ (tube is *on*).

In the relaxation stage, when the capacitor is charging and the tube is off, we have $R_N=\infty$, so that $\dot{V}+(V-E)/CR=0$ and hence $V\to E$ (and slowly, since $RC\gg 1$), but before getting there, it reaches the right endpoint $V=V_+$ provided $V_+<E$, thus

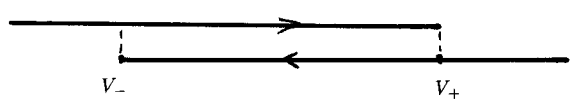

FIG. 2. *Phase flow of equation* (5).

[1] We can, in fact, solve (5) on the linearity intervals for each solution, and derive the shape of the map by estimating the switching points. This approach, however, suffers from two drawbacks: first, it does not explain what is really going on, and second, it cannot be extended to the case when R_N is not a piecewise constant function.

turning on N. Next, the capacitor quickly discharges through N, according to

$$\dot{V}+\frac{1}{C}\left(\frac{1}{R}+\frac{1}{R_c}\right)\left(V-\frac{E}{1+R/R_c}\right)=0,$$

where R_c is the conducting finite value of R_N, so that $V\to E/(1+R/R_c)$, but before getting there it crosses the lower threshold $V=V_-$, if $E/(1+R/R_c)<V_-$, at which point the charging restarts.

As C grows, the period of the limit cycle grows as well.

Let us now consider the *nonautonomous case* of periodic forcing $E_\omega(t)\neq 0$, whose effects on the phase flow are two-fold: first, the discontinuity points $V=V_+ + E_\omega$ of $R_N=R_N(V-E_\omega)$ oscillate and second, $\dot{V}$ has an oscillatory part E_ω/R_N involving a nonlinearity as well. This difficulty of having two simultaneous effects can be resolved by a simple change of variable

$$W=V-E_\omega,$$

which turns (5) into

$$C\dot{W}+\left(\frac{1}{R}+\frac{1}{R_N}\right)W=p(t), \qquad R_N=R_N(W), \tag{6}$$

where the forcing

$$p(t)=\frac{E-E_\omega}{R}-C\dot{E}_\omega$$

is now independent of V. W has the physical meaning: it is simply the voltage on the neon tube.

The difficulty present in (5) has been removed: $p(t)$ is now independent of the phase variables W, $\dot{W}$ and the nonlinearity $R_N(W)$ is independent of t. *The phase flow for W can be obtained from the autonomous flow for V discussed above simply by adding the component $p(t)$.*

3.3. Reduction to a circle map. To analyze the Poincaré map $P: V_{t=0}\to V_{t=T}$, we choose a point V_0 and its iterate $V_1=PV_0$ as the endpoints of the fundamental interval I, which we will call the *window*, since the phase space is "viewed" through it. Assume that I belongs to the upper branch U—this can be achieved by a proper choice of V_0. Define the *return* map $R: I\to I$ as $R(W)=P^j(W)\in I$, where $W\in I$ and $j=j(W)>0$ is the smallest integer for which $P^j(W)\in I$. Identifying V_0 and PV_0 we transform the interval I into a circle and the return map R into a circle map; we keep the same notation I and R. Fixed and periodic points of R are also periodic for P, but the information on the periods of P is lost in R. We will show how to recapture this information in § 3.4. This temporary loss of information is the price for greater simplicity of R in comparison with P.

To analyze the structure of the return map R we trace the evolution of the fundamental interval I with the flow of (6). We only outline the analysis of the window map R; the details can be filled in by using methods similar to [19].

Assume for the purposes of this discussion that $-E_\omega/R-C\dot{E}_\omega>0$ for the first half period $0<t<T/2$ and <0 for the second half-period $T/2<t<T$. Every point in the upper branch U in Fig. 3 undergoes a periodic left-right oscillation superimposed upon a drift to the right, according to the equation $C\dot{W}+W/R=p(t)$. The flow on the lower branch L is so fast to the left—the discharge of C is almost instantaneous for smaller values of C—that it overcomes the oscillations. Starting with the interval I at $t=0$ we observe it moving to the right and stopping[2] at $t=t_{\text{stop}}$ shortly after

[2] Of course, not all points of I stop at the same time, but this can be made precise.

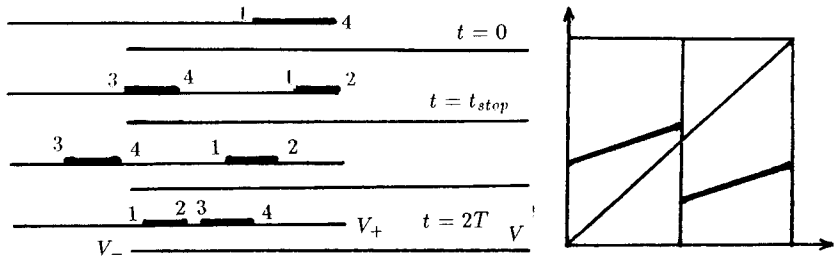

FIG. 3. *Evolution of I with the flow of equation* (6) *and the structure of the window map R.*

$t = T/2$; some point labeled $2 \equiv 3$ lands on the endpoint of the upper branch U (Fig. 3). All points between 3 and 4 had fallen off U and, after a quick trip through L, reappeared on U again (Fig. 3). For the remaining part of the period $t_{\text{stop}} < t < T$, the oscillation is in its leftward phase; the interval I is now torn at $2 \equiv 3$, with both segments (12) and (34) traveling left on U. At $t = T$ the motion stops and reverses direction; before $t_{\text{stop}} + T$ (t_{stop} as defined above) the interval (12) falls off of U and reappears on U again, as shown in Fig. 3 at $t = 2T$. We see that the map P is discontinuous. Tracing the evolution further poses no difficulty: as (12) and (34) drift to the right in an oscillatory fashion, they also contract.

The resulting circle map R together with its graph is depicted in Fig. 3. As we increase C, the images $P^j I$ (j fixed) move left, since larger C result in slower drift (cf. eq. (6)). Equivalently, *the image of the circle map rotates clockwise* (i.e., against the circle's orientation). The change of shape during one rotation is small, in a sense that can be made precise.

3.4. Period-adding. *Each clockwise revolution of the image $R(I)$ due to the change in C results in the increase of the period by* 1—indeed, one clockwise revolution of $R(I)$ is equivalent to the slide of the iterate $P^j(I)$ to the left by the length of one step of the P-iteration, and thus one more P-iteration is required to return to I. This is in complete analogy with the van der Pol-type equation considered below.

3.5. Explanation of the narrowing of the gaps. Van der Pol's and van der Mark's experiments showed that for the capacitance C in the low range the staircase had gaps (Fig. 1(c)). We explain this phenomenon here by tracing more carefully the time-evolution of the window I. For smaller values of C the intervals (12) and (34) return back to I in a smaller number of iterations and thus do not contract by much; as a result the slope of the graph in Fig. 3 is *not much less* than one.

Consequently, there are gaps in C-values for which the return map R is fixed-point free. As C grows, the intervals have more time to shrink, and thus the slope becomes less and the gaps shorten—it is precisely what the experiments show! (Cf. Fig. 1(c).) For C-values in the gaps the map R is fixed point-free, and we must observe higher period fixed points or quasiperiodic or Denjoy behavior [17], which could be misinterpreted as chaos. Indeed, our circle map is order-preserving (although discontinuous) for the lower C-range and thus can exhibit no chaos.

The hysteresis phenomenon can be explained by the fact that for high values of C the window map R becomes noninvertible and acquires two stable fixed points for repeating C-intervals, as seen in Fig. 1(c). The detailed analysis of this effect will be carried out elsewhere.

4. The Poincaré map and the approximating circle map for a class of van der Pol-type equations.

4.1. Preliminary construction. In this section we will summarize the geometrical picture associated with (2). We do so at the heuristic level, avoiding precise statements, to say nothing of the proofs (which are given in [19]). Equation (2) can be conveniently rewritten as a system by setting the modified velocity $y = \varepsilon\dot{x} + \Phi(x)$, where $\Phi(x) = \int_0^x \phi(x)\,dx$:

$$\dot{x} = \frac{1}{\varepsilon}(y - \Phi(x)), \qquad \dot{y} = -\varepsilon x + bp(t). \tag{7}$$

Define the Poincaré (or stroboscopic) map $P: (x, y)_{t=0} \mapsto (x, y)_{t=T}$. Qualitative behavior of (2) is completely captured by the map P.

The map P has the following key geometrical properties (for the proper parameter values, namely, for $\varepsilon > 0$ small enough (and fixed) and for the forcing amplitude b between 0 and $2m/\bar{p}$, not too close to the endpoints, where m = local maximum of $\Phi(x)$ and $\bar{p} = \int_0^T p_+(t)\,dt = \int_0^T p_-(t)\,dt$):

- The map P has exactly two fixed points, one at infinity and another z_0, close (for small ε) to the negatively sloped branch of $y = \Phi(x)$ (Fig. 4).

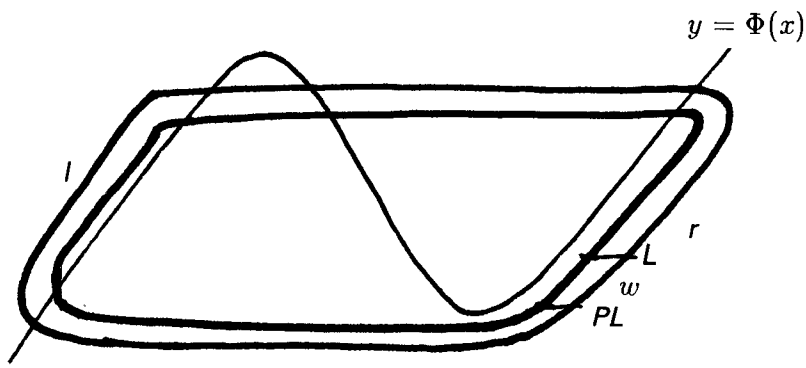

FIG. 4. *Vertical dimension of the annulus* $A \approx 2m - b\bar{p}$.

- Attractor of P lies entirely inside an annulus A of thickness $< \sqrt{\varepsilon}$, sketched in Fig. 4. That is, any point $z \neq z_0$ or ∞ enters A and stays there after sufficiently many iterations by P.
- The points in A "circulate clockwise" under P-iterates. More precisely, the right side r of A is (roughly speaking) contracted in the horizontal direction by $\sim e^{-1/\varepsilon}$ and translated downward along the branch of Φ by $O(\varepsilon)$. The lower part of r of length $O(\varepsilon)$ spills partly to the bottom and partly to the left part l of the annulus. Similar statements hold for the left part l.

The evolution of points is quite simple as long as they stay in l or r; *it is the transition from l to r and from r to l that is responsible for the interesting dynamics of the system.*

Remark. A superficial glance at period-adding. At this point our description of the map is still extremely sketchy, but already we can give a heuristic indication of the occurrence of period-adding. The total circumference of the annulus A depends nearly linearly on b, whereas the average size of step under P-iterations is virtually independent of b by comparison. Thus the number of P-iterations it takes for the point to complete one trip around A decreases with b; in particular, periods of periodic points could be expected to decrease with b.

4.2. Reduction to a simple circle map. Now we give a more precise description of the map P; it turns out to be of a surprisingly simple form in the end. We construct a region w (in Fig. 4), which we will call the window, bounded by the two sides of r and by a horizontal line L joining the vertical boundaries of r and its image Pl.

The crucial property of w is that iterates of any point $z \neq z_0$ pass through w, and hence do so repeatedly. It suffices, therefore, to trace the evolution of w under P-iterations. This evolution is the central part of understanding the dynamics of the system; it is depicted in Fig. 5(a), where the positions of w at *different times* are shown.

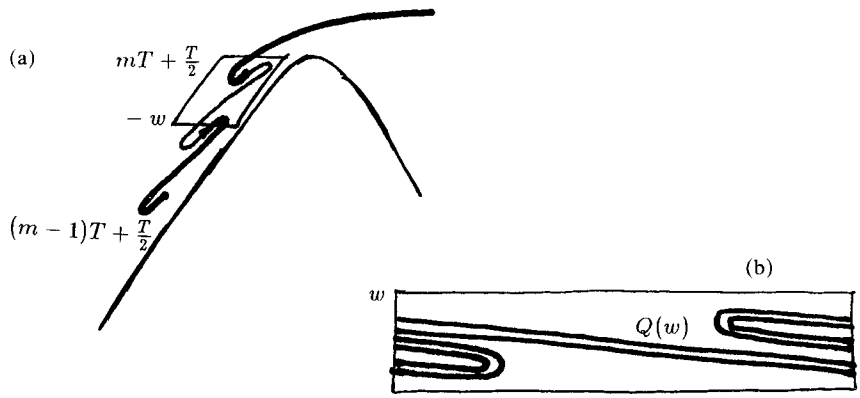

FIG. 5. (a) *Evolution of the window w with time.* (b) *The antipodal return map defined by* $Q(z_0) = -Z(mT + T/2, 0, z_0)$; $Q^2 = R$.

To determine the qualitative behavior of the Poincaré map P we must determine how future iterates of the window w intersect w. To that end, we consider the window map $R: w \to w$ defined by $z \to P^j z \in w$ where $j = j(z) > 0$ is the smallest integer for which the last inclusion holds. The only piece of information we lose by considering R instead of P is the integer-valued function $j(z)$, so we will keep track of it. The advantage of looking at the window map R instead of P lies in the (as yet nonobvious) simplicity of the reduced map. This simplicity is further enhanced by the symmetry properties of the damping and forcing functions $\phi(x)$ and $p(t)$, which imply that the window map R is the second iterate of the "antipodal half-period return map" Q (of even simpler form); we have the following lemma.

LEMMA. $R = Q \circ Q = Q^2$, *where the map* $Q: w \to w$ *is defined for any* $z \in w$ *as* $Q(z) = -Z(mT + T/2, 0, z) \in w$, *with* $Z(t, t_0, z)$ *denoting the solution of* (3) *at time* t *which starts at* z *at time* t_0, *and where* $m = m(z) > 0$ *is the smallest integer for which the last inclusion holds.*

Proof of this lemma is given in the Appendix.

The "square root" Q of the window map R has a surprisingly simple form, shown in Fig. 5(b).

The choice of the window makes it natural to turn Q into an *annulus map* as follows. The map Q is discontinuous, since the integer $m(z)$ experiences jumps: a point $z' \in w$ near $z \in w$ may require one more (or one less) period T to reach $-w$. This will be the case for precisely those points $z \in w$ that land on the top or the bottom boundaries of $-w$ at some odd multiple $mT + T/2 = (2m+1)T/2$ of $T/2$. By identifying the corresponding points on these boundaries we remove the discontinuity, while at the same time turning w into an annulus; this is why we represent Q by an annulus map. Since w is an extremely thin region for ε small (of width $\sim e^{-c/\varepsilon^2}$), the annulus

map Q can be closely approximated by the one-dimensional circle map $\hat{Q}$ shown in Fig. 6.

The *b-dependence of* Q is surprisingly simple as well. Roughly speaking, as b grows, the vertical size $2m - b\bar{p}$ of A decreases; meanwhile, the size of the folds in Fig. 5 remains nearly constant. This means that as b grows (from 0 to $2m/\bar{p}$) *the folds travel upward through the window* w; this translates into the statement: *as* b *grows, the image* $Q(w)$ *rotates clockwise* (with angular velocity $\sim 1/\varepsilon$).[3] Each full turn of the graph of Q amounts to the change of the integer m by one. This statement translates for the circle map $\hat{Q}$ in the obvious way.

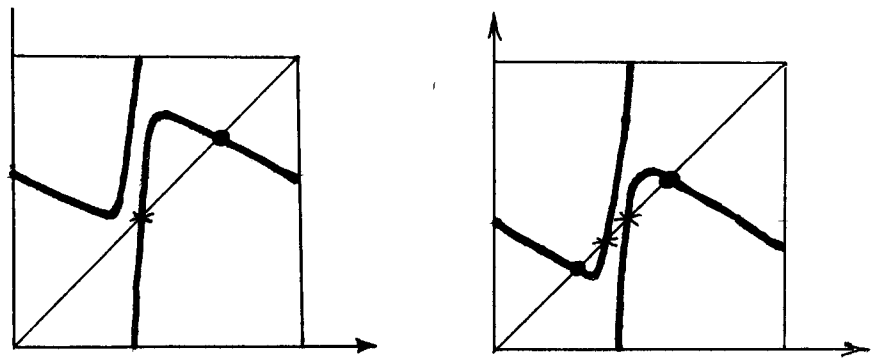

FIG. 6. *Circle map* $\hat{Q}$ *for different parameter values. Stable fixed points (marked by circles) for* $\hat{Q}$ *correspond to the sinks for the two-dimensional map* Q*, while the unstable fixed points of* $\hat{Q}$ *correspond to the saddles of* Q.

The next section contains the explanation of the geometrical cause of period-adding for (2).

5. Explanation of period-adding and of other dynamical phenomena in a class of van der Pol-type equations.

5.1. Period-adding and the "Angel's staircase." As b increases (by an amount on the order $O(\varepsilon)$), the image $Q(w)$ undergoes one clockwise revolution (plus some minor distortion); correspondingly, one less fold fits between w and $-w$ (going clockwise) in Fig. 3; equivalently, the corresponding points from w will require one more period to get to $-w$, and two more to return to w. This explains the "Angel's staircase."

5.2. Odd periods. Briefly put, odd periods are due to the existence of the factorization $R = Q \circ Q$ (which in turn follows from symmetry properties of $\phi(x)$ and $p(t)$). More precisely, let z_0 be a fixed point for Q; this amounts to the fact that it takes time $mT + T/2$ to get from z_0 to $-z_0$, starting at $t = 0$, and furthermore (by symmetry), it takes the same time to get from $-z_0$ back to z_0, starting on the half-period. Summarizing, it takes time $2 \times (mT + T/2) = (2m+1)T$ for the point z_0 to make one full revolution and to return to its initial position, which explains the oddness of the period of the periodic solutions observed in the van der Pol's equation.

5.3. Noise. The noise observed in the van der Pol system can be explained by the appearance of Henon-like attractors for Q for special values of $b \in C_n$. That such attractors should appear is clear from Fig. 5, where the position of the fold can be controlled by b. Actually, for numerical purposes these attractors are one-dimensional, and more can be said about them.

[3] The exact picture is, of course, much more complex in its details [19].

For small ε the map Q is closely approximated by a circle map; in fact, for $\varepsilon = .2$ the difference is indistinguishable in double precision, and for numerical purposes we can treat Q as a circle map. Jakobson's results [15] on certain "typical" families of one-dimensional maps provide the existence of absolutely continuous invariant measures for "many" parameter values. This will be manifested as noise for the equation. Actually, for smaller ε strange attractors for Q are confined to a very small subset; this is due to the fact that the folds in the graph of $\hat{Q}$ became sharp for small ε [19]. This noise is, in fact, hard to observe numerically, as confirmed by the experiments by Flaherty and Hoppensteadt [7].

It should be emphasized that the mere presence of the horseshoes does *not* imply noise, for instance, for $b \in B_n$ the Poincaré map P possesses a horseshoe, corresponding, however, to a zero measure set in the (x, y)-plane.

5.4. Devil's staircase embedded in the "Angel's staircase." Using the picture associated with the circle map $\hat{Q}$, it is easy now to explain the reason for the steplike character of the dependence of the rotation number on b. As the parameter b grows from 0 to $2m/\bar{p}$, the circle map will have alternately one sink for the A-intervals of parameter and two sinks for the B-intervals of b. The corresponding solutions will have odd periods $(2n+1)T$ in the intervals A_n and $(2n \pm 1)T$ in the intervals B_n; the rotation numbers for these solutions are given by $1/(2n \pm 1)$ and are plotted in Fig. 1(d).

Bifurcations in the gaps. No experimental data are available for the bifurcations of (1) or (2) in the gaps C_n; we discuss some predictions from the general theory as applied to the system in question, and mention a possible explanation of secondary staircases observed in the circuit by Chua, Yao, and Yang [6]. Assume that $b \in B_n$ begins to increase, entering the gap C_{nl}. During the passage of b through the gap, the interval of rotation numbers shrinks from $[1/(2n+1), 1/(2n-1)]$ to the point $1/(2n+1)$; the left endpoint of the interval remains fixed throughout the gap, *whereas the right endpoint's evolution is given by the devil's staircase.* When the endpoint is rational (which is the case for an open interval of b-values), it serves as the rotation number of a stable periodic orbit. These orbits will be of period higher than the lowest possible period $2n-1$. It is most likely that precisely this phenomenon is responsible for the secondary and higher staircases observed in the above quoted paper [6]. It must be pointed out that the gaps contain, among other things, the period-doubling sequence.

5.5. Rotation numbers and symbolic dynamics. For $b \in B_n$ the set of *all* rotation numbers forms *precisely* the interval $[1/(2n+1), 1/(2n-1)]$. This was proven in [19, p. 71] by using symbolic description of the map Q for $b \in B_n$. The idea of the proof was to find an invariant Cantor set whose points correspond to bi-infinite sequences $\{\sigma_j\} = \pm 1$ and to observe that the rotation number $r(z)$ of the point z is given by the mean value ρ of this sequence: $r = 1/(2n+\rho)$ where

$$\rho = \lim_{n \to \infty} \sum_{j=1}^{j=n} \sigma_j.$$

Given an *arbitrary* number $\rho \in [-1, 1]$ we can create an *uncountable* set of sequences of ± 1 with that average;[4] consequently, there is an uncountable number of points with any given rotation number in the interval $[1/(2n+1), 1/(2n-1)]$. In fact, we can speak of both forward and backward rotation numbers, which can be arranged independently: for each pair of numbers r_+, r_- from the above interval there exists a point with r_+, r_-

[4] It suffices to observe that ρ does not change even if an infinite subsequence σ_{j_k} of σ_n is altered arbitrarily, provided the subsequence has zero density: $k/j_k \to 0$ as $k \to \infty$.

as the forward and backward rotation numbers. In fact, there is an uncountable set of such points, as we noted above.

The points in the Cantor set form the boundary between the basins of two attracting periodic orbits of periods $(2n \pm 1)$; these points cannot decide which of the two attractors to approach, and they hesitate in their choice in a rather arbitrary way, according to the symbols σ_j, leading to the nonuniqueness of rotation numbers.

For many (in some sense most) points in the Cantor set the rotation number actually fails to exist—this is equivalent to the statement of the nonexistence of the average value ρ.

An extensive computer-based study of basin boundaries has been carried out by Grebogi, Ott, Yorke, and others.

5.6. Monotone twist maps. The aim of this short paragraph is to show how to apply some recent results in Aubry-Mather theory [1], [2], [4], [5], [11], [12], [14], [22]-[24] to (2). Poincaré map P turns out to be a monotone twist map (in proper coordinates), as follows from the analysis of the linearized equations in [19]. Applying the topological version of the Aubry-Mather Theorem [22] due to Hall [11] and Bernstein [2], we conclude the existence of "minimal energy" orbits for any rotation number between $1/(2m+1)$ and $1/(2m-1)$; in our case, the minimality is not metric but topological: in a proper projection, the orbits are ordered as iterates of an invertible circle map. One can specify symbolic sequences for the horseshoe map corresponding to such orbits, using the results of [3], [8], [13].

Hall's topological version [12] of Mather's variational shadowing theorem applies in our case as well, giving information on the nonwell-ordered orbits. According to this theorem, for any sequence of periodic orbits there exists an orbit that shadows each sequence for a prescribed number of iterations. We refer to [12] for the precise statement.

We remark finally, that for $b \in B_n$ the two stable periodic orbits of periods $1/(2m+1)$, $1/(2m-1)$ are *linked.* According to a theorem by Boyland [4] the rotation set includes the interval $[1/(2m+1), 1/(2m-1)]$, and furthermore, for any rotation number p/q from that interval there exists a Birkhoff periodic orbit with that rotation number.

Full analysis of the map has been obtained earlier by analytical methods, but these topological theorems that have since appeared allow us to obtain partial information without full analysis, using only the monotone twist property and the linking property.

Remark. The above description allows for the virtually complete analysis of the behavior of (3), of its bifurcations, etc. [19] (see also Guckenheimer and Holmes [10]). Equation (1), in spite of its apparent simplicity, exhibits virtually all the phenomena found in the mappings of the plane: horseshoes, Newhouse sinks, homoclinic bifurcations, Henon-type attractors, Aubry-Mather sets (in the dissipative setting), etc.

Appendix. Proof of the Lemma $R = Q \circ Q$.

Step 1. Define the "half-period antipodal" map S by $S(z) = -Z(T/2, 0, z)$, and prove first that $P = S \circ S \equiv S^2$. This follows from (A1) and (A2) below:

$$\text{(A1)} \qquad Z(t, 0, z) = -Z\left(t + \frac{T}{2}, \frac{T}{2}, -z\right);$$

to prove this, we observe that both sides of (A1) are solutions of (7) by the symmetry properties of ϕ and furthermore, they satisfy the same initial conditions so that (A1)

holds by uniqueness of solutions. Furthermore, we have

$$Z(t, t_1, Z(t_1, t_0, z)) = Z(t, t_0, z), \tag{A2}$$

for any $t_0, t_1, t \in \mathbf{R}$ and any $z \in \mathbf{R}^2$. To prove this we note again that both sides of (A2) are solutions of (eq. (7)), which moreover coincide for $t = t_1$, and hence for all t.

Substituting $t = T/2$ in (A1) we obtain

$$Z\left(\frac{T}{2}, 0, z\right) = -Z\left(T, \frac{T}{2}, -z\right); \tag{A1}'$$

setting $t_0 = 0$, $t_1 = T/2$, $t = T$ in (A2), we obtain

$$Z\left(T, \frac{T}{2}, Z\left(\frac{T}{2}, 0, z\right)\right) = Z(T, 0, z), \tag{A2}'$$

or, by the definitions of P and S:

$$Z\left(T, \frac{T}{2}, -S(z)\right) = P(z).$$

Applying (A1)′ to the left-hand side, we get the desired factorization

$$S(S(z)) = P(z).$$

Step 2. Define $Q = S^{2m+1}$, where $m = m(z)$ is an integer-valued function defined for each $z \in w$ as the smallest integer >0 for which $S^{2m+1}z \in w$. We note that $Qz = S^{2m+1}z = -Z(mT + T/2, 0, z)$, as follows from Step 1. Indeed,

$$Qz = S^{2m+1}z = S \circ S^{2m}z = S \circ P^m z = S(Z(mT, 0, z)) = -Z\left(mT + \frac{T}{2}, 0, z\right).$$

This, together with Fig. 3(a), makes it clear that $Q: w \to w$ is well-defined.

To complete the proof of the lemma, we break up R as follows. For any $z \in w$

$$Rz \overset{\text{def}}{\equiv} P^j z \overset{\text{step 1}}{\equiv} S^{2j}z = S^{2(j-m)-1}(S^{2m+1}z) = S^{2(j-m)-1}(Qz) \in w,$$

and since $Qz \in w$, we have $2(j - m(z)) - 1 = m(Qz)$, so that $R = Q \circ Q$. □

REFERENCES

[1] S. AUBRY AND P. Y. LEDAERON, *The discrete Frenkel-Kontorova model and its extensions* I: *Exact results for the ground states*, Phys. D, 8 (1983), pp. 381-422.

[2] D. BERNSTEIN, *Birkhoff periodic orbits for twist maps with the graph intersection property*, Ergodic Theory Dynamical Systems, 5 (1985), pp. 531-537.

[3] C. BERNHARDT, *Rotation intervals for a class of endomorphisms of the circle*, Proc. London Math. Soc. 3, 45 (1982), pp. 258-280.

[4] P. L. BOYLAND, *Invariant circles and rotation bands in twist maps*, Comm. Math. Phys., 113 (1987), pp. 66-77.

[5] P. L. BOYLAND AND G. R. HALL, *Invariant circles and the order structure of periodic orbits in monotone twist maps*, Topology, 26 (1987), pp. 21-35.

[6] L. O. CHUA, Y. YAO, AND Q. YANG, *Devil's staircase route to chaos in a nonlinear circuit*, Circuit Theory Appl., 14 (1986), pp. 315-329.

[7] L. E. FLAHERTY AND F. C. HOPPENSTEADT, *Frequency entrainment of a forced van der Pol oscillator*, Stud. Appl. Math., 18 (1978), pp. 5-15.

[8] J.-M. GAMBAUDO, O. LANFORD III, AND C. TRESSER, *Dynamique Symbolique des Rotations*, C.R. Acad. Sci. Paris Ser. 1, 16 (1984), pp. 823-826.

[9] J. GRASMAN, *Relaxation oscillations of a van der Pol equation with large critical forcing term*, Quart. Appl. Math., 38 (1980), pp. 9-16.

[10] J. GUCKENHEIMER AND P. HOLMES, *Nonlinear oscillations, dynamical systems and bifurcations of vector fields*, Springer-Verlag, Berlin, New York, 1983.

[11] G. R. HALL, *A topological version of a theorem of Mather on twist maps*, Ergodic Theory Dynamical Systems, 4 (1984), pp. 585-603.

[12] ———, *A topological version of a theorem of Mather's on shadowing in monotone twist maps*, in Proc. of Semester in Dynamical Systems, Banach Inst., Warsaw, to appear.

[13] K. HOCKETT, *Locating the well-ordered periodic points of the angle doubling map on* S^1, preprint.

[14] K. HOCKETT AND P. HOLMES, *Josephson's junction, annulus maps, Birkhoff attractors, horseshoes and rotation sets*, Ergodic Theory Dynamical Systems, 6 (1986), pp. 205-239.

[15] M. V. JAKOBSON, *Absolutely continuous invariant measures for one-parameter families of one-dimensional maps*, Comm. Math. Phys., 81 (1981), pp. 39-88.

[16] K. KANEKO, *On the period-adding phenomena at the frequency locking in a 1-dimensional mapping*, Progr. Theoret. Phys., 68 (1982), pp. 669-672.

[17] J. P. KEENER, *Chaotic behavior in piecewise continuous difference equations*, Trans. Amer. Math. Soc., 261 (1980), pp. 589-603.

[18] M. P. KENNEDY AND L. O. CHUA, *van der Pol and chaos*, IEEE Trans. Circuits and Systems, 33 (1986), pp. 974-980.

[19] M. LEVI, *Qualitative analysis of the periodically forced relaxation oscillations*, in Mem. Amer. Math. Soc. 244, Providence, RI, 1981.

[20] J. E. LITTLEWOOD, *On non-linear differential equation of second order*: IV, Acta Math., 98 (1957), pp. 1-110.

[21] J. MASELKO AND H. L. SWINNEY, *Complex periodic oscillations and Farey arithmetic in the* B-Z *reaction*, J. Chem. Phys., 85 (1986), pp. 6430-6441.

[22] J. N. MATHER, *Existence of quasi-periodic orbits for twist homeomorphisms of the annulus*, Topology, 21 (1982), pp. 457-476.

[23] ———, *More Denjoy minimal sets for area-preserving diffeomorphisms*, Comment. Math. Helv., 60 (1985), pp. 508-557.

[24] J. K. MOSER, *Break-down of stability*, Lecture Notes in Physics 247, J. M. Jowett, M. Month, and S. Turner, eds., Springer-Verlag, Berlin, New York, 1986, pp. 492-518.

[25] L.-Q. PEI, F. GUO, S.-X. WU, AND L. O. CHUA, *Experimental confirmation of the period-adding route to chaos in a nonlinear circuit*, IEEE Trans. Circuits and Systems, 33 (1986), pp. 438-442.

[26] A. S. PIKOVSKY, *A dynamical model for periodic and chaotic oscillations in the Belousov-Zhabotinsky reaction*, Phys. Lett. A, 85 (1981), pp. 13-16.

[27] I. TSUDA, *Self-similarity in the Belousov-Zhabotinsky reaction*, Phys. Lett. A, 85 (1981), pp. 4-8.

[28] J. S. TURNER, J.-C. ROUX, W. D. MCCORMICK, AND H. L. SWINNEY, *Alternating periodic and chaotic regimes in a chemical reaction—experiment and theory*, Phys. Lett. A, 85 (1981), pp. 9-12.

[29] VAN DER POL AND J. VAN DER MARK, *Frequency demultiplication*, Nature, 120 (1927), pp. 363-364.